

# Single-Polymer Friction Force Microscopy of dsDNA Interacting with a Nanoporous Membrane

Published as part of Langmuir *virtual special issue* “2023 Pioneers in Applied and Fundamental Interfacial Chemistry: Nicholas D. Spencer”.

Kordula Schellnhuber, Johanna Blass, Hanna Hübner, Markus Gallei, and Roland Bennewitz\*

Cite This: *Langmuir* 2024, 40, 968–974

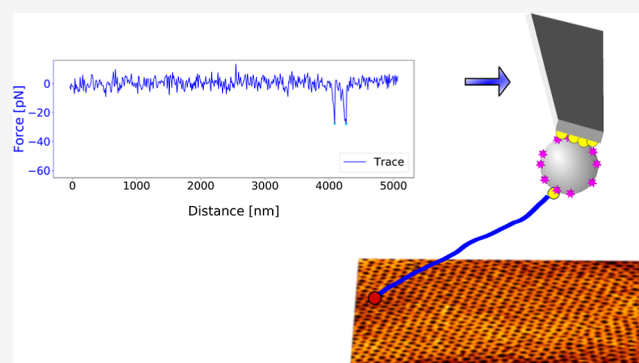
Read Online

ACCESS |

Metrics & More

Article Recommendations

**ABSTRACT:** Surface-grafted polymers can reduce friction between solids in liquids by compensating the normal load with osmotic pressure, but they can also contribute to friction when fluctuating polymers entangle with the sliding counter face. We have measured forces acting on a single fluctuating double-stranded DNA polymer, which is attached to the tip of an atomic force microscope and interacts intermittently with nanometer-scale methylated pores of a self-assembled polystyrene-*block*-poly(4-vinylpyridine) membrane. Rare binding of the polymer into the pores is followed by a stretching of the polymer between the laterally moving tip and the surface and by a force-induced detachment. We present results for the velocity dependence of detachment forces and of attachment frequency and discuss them in terms of rare excursions of the polymer beyond its equilibrium configuration.



## INTRODUCTION

Polymer brushes grafted onto surfaces are excellent lubricants in good solvents. Osmotic pressure leads to repulsive forces when the brushes on opposing surfaces are compressed and keeps the surfaces separated as long as the applied load is limited.<sup>1</sup> The remaining shear stress between the brushes arises from the viscous drag between interpenetrating polymers when the two brushes overlap under an increasing load. The analysis of bead–spring simulations revealed an onset of shear force when the interpenetration reaches the size of at least one spherical blob with radius  $\sqrt{\rho_a}$ , the square root of the coverage of surfaces with polymer forming the brush.<sup>2</sup>

Nicholas D. Spencer, who is honored with this virtual issue of Langmuir, has made important contributions to our understanding of lubrication by polymer brushes or surface-attached hydrogels. He introduced PLL-*g*-PEG as a lubricating brush in aqueous solvents which is easily applied to oxide surfaces and exhibits load-bearing capacity in experiments at different length scales.<sup>3–5</sup> He has shown that the entropic effects which limit the interpenetration of polymers are reduced in poorer solvents.<sup>6</sup> Additionally, his work on surface-attached hydrogels has shown that the density of dangling polymers at the interface affects shear forces not only via interpenetration but also through modulation of hydrodynamic lubrication.<sup>7,8</sup>

Spencer’s initiatives to study polymer brush lubrication also at small length scales and to reveal microscopic mechanisms related to the polymer architecture<sup>9,10</sup> has inspired us to extend single-molecule force spectroscopy to friction studies. Here, we report the results of an idealized experiment to study lateral forces of a single polymer which is attached to a force probe and moved along a nanoporous surface at a constant height (see Figure 1). The single polymer is a double-stranded DNA construct (dsDNA) which we choose for its defined length and its well-studied mechanical properties.<sup>11,12</sup> The goal of the study is to establish an experimental technique for quantifying the contribution of a single fluctuating polymer to friction, where the polymer intermittently interacts with pores or meshes of the surface, in our study, a flat nanoporous membrane.<sup>13</sup>

The feasibility to study the friction of single polymers by atomic force microscopy (AFM) has been demonstrated previously.<sup>14–16</sup> Analysis of force curves recorded in water

**Received:** October 20, 2023  
**Revised:** December 1, 2023  
**Accepted:** December 11, 2023  
**Published:** December 20, 2023



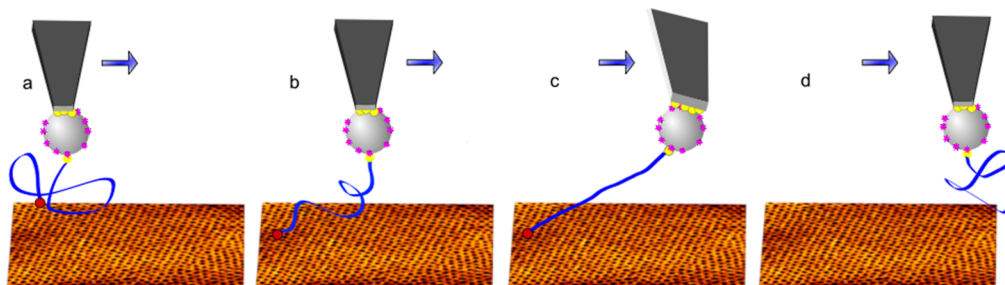


**Figure 1.** Schematic representation of the experiment. (a) Double-stranded DNA molecule with a contour length of 2500 nm is attached to a colloidal AFM probe, which moves laterally at a height of 250 nm over a nanoporous membrane in a physiological buffer solution. (b) Fluctuating end of dsDNA eventually attaches to the membrane surface, presumably by interacting with a methylated pore. (c) Molecule is uncoiled and stretched as the cantilever is moving on. (d) dsDNA molecule is detached by the increasing force acting on its bond to the surface. The scanning motion of the AFM probe is repeated line by line in both directions with a scan width of twice the contour length, while detachment forces are recorded.

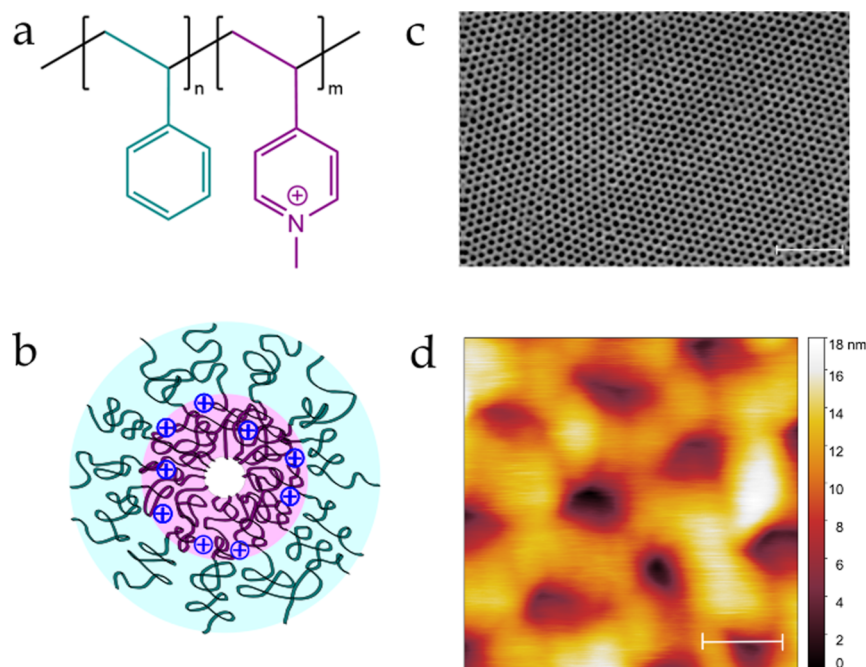


**Figure 2.** Composition and structure of the nanoporous membrane. (a) Structure formula of the block copolymer consisting of PS and methylated P4VP. (b) Scheme of a single pore as part of the block copolymer membrane consisting of a PS matrix and positively charged pore walls of methylated P4VP. The porous membrane was methylated in order to form the positively charged pyridinium moieties. (c) SEM of the integral asymmetric block copolymer membrane after application of the SNIPS process. The pores are distributed homogeneously in domains of hexagonal arrangement. (Scale bar = 500 nm). (d) Topography of the membrane recorded by AFM. (Scale bar = 50 nm).

on PTFE revealed how different polymers may either slide in contact, resist sliding by cooperatively sticking to one position, or undergo a simultaneous sticking and desorption.<sup>14</sup> The high force resolution of experiments under vacuum even allowed us to reveal atomic mechanisms of the sliding of a graphene nanoribbon over a crystalline surface.<sup>16</sup>

Our experiment extends these studies by including the role of polymer fluctuations and random surface attachment and investigates the contribution to friction as stretching due to lateral sliding and forced detachment. It thus provides a framework for studying the fundamental mechanisms of hydrogel friction from a molecular perspective.

## EXPERIMENTAL SECTION

For our experiment, we needed to attach a single polymer of well-defined length to the cantilever of an atomic force microscope. Furthermore, we need to prepare a flat substrate with nanometer-scale

roughness that offers meshes or pores for a measurable intermittent interaction with the polymer. For our study, we choose the interaction of a negatively charged dsDNA in physiological buffer [phosphate-based solution phosphate buffer (PBS) with pH 7.4] with the positively charged walls of methylated nanopores in a self-assembled membrane. In the following, we will describe the preparation of the nanoporous membrane, the hybridization and functionalization of DNA molecules, the attachment of single dsDNA molecules to the tip of the atomic force microscope, and the single-molecule friction force experiment.

**Nanoporous Membrane with Charged Pore Walls.** The nanoporous membrane was prepared by a self-assembly and nonsolvent-induced phase separation (SNIPS) process of amphiphilic polystyrene-*block*-poly(4-vinylpyridine) polymers (Figure 2a) following the procedures reported in ref 13. The self-assembly process creates a flat membrane that consists of a polystyrene (PS) matrix and an ordered array of nanopores formed by walls of poly(4-vinylpyridine) (P4VP) polymer segments (Figure 2b,c). This nanoporous membrane has a thickness of about 200 nm and is

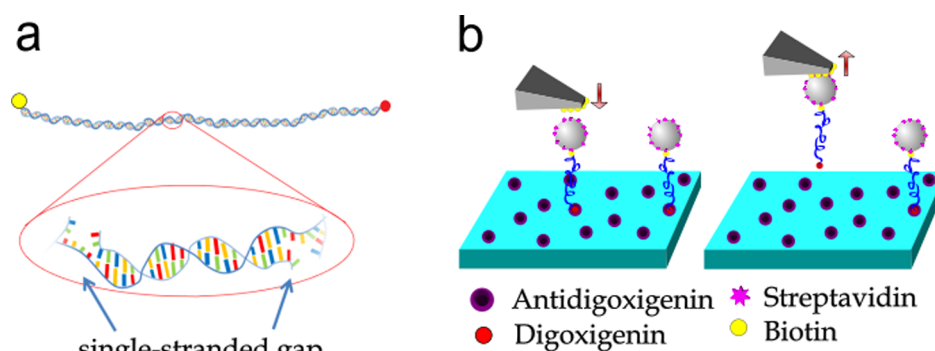


**Figure 3.** Details of the dsDNA preparation. (a) Single-stranded DNA molecule (7198 nts) is hybridized by 123 oligomers with complementary base pairs to create a double-stranded helix. Nicks are formed in gaps between the oligomers. The dsDNA molecules are functionalized at the ends with digoxigenin and biotin for attachment to different surfaces. (b) dsDNA molecules are attached to a glass slide using the digoxigenin–antidigoxigenin bond. A bead coated with streptavidin is attached to the other end of dsDNA. In order to attach a single dsDNA molecule to the atomic force microscope cantilever, a bead is located by optical microscopy and the biotin-coated cantilever approached to form a strong bond between the bead and cantilever. When the cantilever is retracted, dsDNA is pulled off the surface.

supported by a sponge-like irregular substrate of the same material. Subsequent to the membrane assembly, the internal walls of the nanopores were equipped with a positive charge by quaternization of the nitrogen atoms in the P4VP molecules via gas-phase methylation.<sup>17</sup> The mean distance between pores is  $74 \pm 4$  nm; the pore diameter can only be estimated from scanning electron microscopy (SEM, Figure 2c) and AFM images (Figure 2d) to be around 40 nm. The root-mean-square roughness of the membrane measured by AFM on a lateral length scale of  $5 \mu\text{m}$  is of the order of 5 nm. The roughness value is dominated by the penetration of the atomic force microscope tip into the pores of the membrane, whose overall roughness is even smaller.

**DNA Hybridization and Functionalization.** The double-stranded DNA construct is prepared following a previously reported DNA self-assembly protocol.<sup>12</sup> In summary, the circular single-stranded M13mp18 plasmid (New England Biolabs) is linearized by the BtsCI restriction enzyme (New England Biolabs) after hybridizing with a 40 nt oligomer to define the double-stranded restriction site. The double-stranded DNA construct of 7198 nts is then created by hybridizing 123 complementary oligomers, most of them with 60 nts, in 10-fold excess to a 15 nM solution of the linearized scaffold DNA. To allow for a specific binding of the dsDNA molecules, one end was functionalized with biotin and the other end with digoxigenin. These binding motifs were attached by hybridization of functionalized oligomers. The self-assembly is carried out in a thermocycler with a temperature ramp from 90 to 20 °C with a cooling rate of 1 °C/min. The DNA construct is stored at 4 °C for immediate use or at –20 °C for later use. Please note that hybridization with 60 nts oligomers results in a fully double-stranded DNA with a contour length of  $L_0 = 7198 \times 0.34 \text{ nm} = 2448 \text{ nm}$ , but that the complementary strand is disconnected every 60 nucleotide positions (Figure 3a). The corresponding nicks in dsDNA reduce the effective persistence length to  $P = 10.3 \text{ nm}$ .<sup>12</sup>

**Attachment of Single dsDNA Molecules to the Atomic Force Microscope Cantilever.** To attach single dsDNA molecules to the atomic force microscope cantilever, we first use the molecules to tether micrometer-sized beads to a surface at low density. We then pick up the beads by the atomic force microscope cantilever and with them the dsDNA molecules as visualized in Figure 3b. This method makes single-molecule attachment highly probable, first by binding DNA molecules to an excess of beads and then by selecting those beads for pick-up which exhibit the symmetric Brownian motion of single-molecule tethering. Bead pick-up and friction experiments were performed in a NanoWizard3 AFM (jpk Instruments, Berlin, Germany) mounted on an inverted optical microscope (Zeiss Axio Observer).

To bind single dsDNA constructs to the beads by means of the biotin-streptavidin interaction, a 5 pM solution of the dsDNA

construct in PBS is mixed with a 10-fold excess of streptavidin-covered microbeads (Dynabeads MyOne C1 from Thermo Fisher). To tether the beads to a surface by means of the dsDNA molecules, a glass slide is functionalized with antidigoxigenin. The protocol comprises coating the glass slide with a nitrocellulose layer, incubating antidigoxigenin solution, and passivating the surface by a blocking reagent. A droplet of DNA-bead solution is placed on the surface to bind dsDNA with the digoxigenin-antidigoxigenin bonds. Untethered beads are removed by rinsing with PBS. All details can be found in ref 12.

The beads with dsDNA are picked up by a tipless, triangular cantilever (MLCT-O10, Bruker), which was coated with biotinylated albumin (Sigma-Aldrich, immersion overnight in 0.5 mg/L). Beads that are tethered by single DNA molecules are identified by their symmetric Brownian motion in optical microscopy. The cantilever is moved over the bead and approached the contact for a dwell time of 1 s. Multiple biotin groups on the cantilever bind to streptavidin binding sites exposed on the bead and form a bond stronger than the single antidigoxigenin–digoxigenin bond which keeps the DNA attached to the surface. Several force–distance curves on the antidigoxigenin-coated surface are recorded to verify the attachment of a single DNA construct through observation of characteristic rupture events at a distance of more than  $2 \mu\text{m}$  from the surface, as shown and discussed in ref 12.

**Friction Measurements.** For the friction measurements, the cantilever with the attached dsDNA construct is moved to the nanoporous membrane. Forces were recorded while the tip was scanning back and forth at a height of 250 nm and over a lateral distance of  $5 \mu\text{m}$ . The height is chosen larger than the expected equilibrium size of the coiled dsDNA molecule but small enough to allow for surface interaction when the fluctuating molecule extends beyond its equilibrium size. The height was controlled by moving the tip into contact every 100 scan lines, or when the scanning velocity was changed. Furthermore, the height was monitored during experiments by means of the capacitive distance sensor integrated in the atomic force microscope head. Normal forces acting on the cantilever are measured by recording the vertical deflection of the cantilever with the beam-deflection scheme of the atomic force microscope. While we would prefer to also record lateral forces exerted by the molecule on the cantilever, the atomic force microscope's sensitivity to detect lateral forces as cantilever twisting is too low for the pN range of forces in single-molecule force microscopy.<sup>14</sup>

## RESULTS AND DISCUSSION

Friction force microscopy with a single, fluctuating polymer was successfully established in physiological buffer; it can therefore be applied to biomaterials in future experiments.



Figure 4 shows typical force traces. Single force peaks are preceded, with respect to the scanning direction, by a

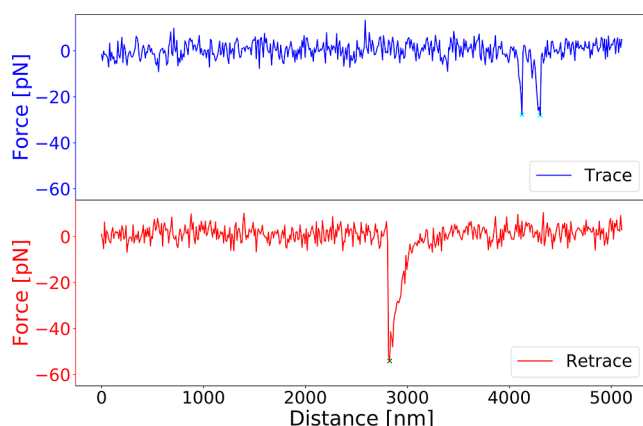


**Figure 4.** Exemplary force traces recorded while the atomic force microscope tip was scanning at a height of 250 nm over the nanoporous membrane. Characteristic isolated peaks indicate the intermittent attachment, stretching, and force-induced detachment of the single DNA molecule. In total, three detachment events are shown, two during the trace (blue) and one during the retrace scan (red).

nonlinear increase of the force as a function of distance. The curve shape of each event indicates the stretching of the dsDNA molecule and finally detachment from the surface. The wormlike chain model predicts for our dsDNA construct that its linear entropic extension is hidden in the force noise of our experiment. At a force of 5 pN, the molecule is already extended to 2400 nm, 97% of its contour length. We conclude that the molecule is intermittently attached to the surface and then stretched until the force is high enough to rupture the bond. Balzer et al. have described this type of single-molecule friction as the result of cooperative stick of the polymer to the surface, in contrast to a possible sliding of the attached polymer or a desorption stick, where the polymer is peeled of the surface under increasing force.<sup>14,18</sup> Most detachment events had rupture forces between 20 and 60 pN, but few ruptures occurred at values up to 200 pN.

To further characterize the surface bond, we performed the experiments at different sliding velocities and plot the median rupture force as a function of the force pulling rate in Figure 5a. The low signal-to-noise ratio in our data and the unknown

projection of the acting force on the normal direction probed by the cantilever did not allow for the determination of force pulling rates for each single rupture event. Therefore, the force pulling rate was estimated as the product of scanning velocity and spring constant. We attributed a detachment event to a force peak if the maximum force exceeded the root-mean-square force noise by a factor of 3.5. The logarithmic dependence of the rupture force on the force-loading rate as observed in Figure 5a is often reported and analyzed in single-molecule force spectroscopy.<sup>19</sup> Given the limited range of pulling rates and the uncertainties in their determination, we refrain from further analysis of the bond strength or kinetics. The logarithmic dependence on the pulling rate still allows us to conclude that the lifetime of the bond is long compared to typical experimental time scales, namely, the contour length divided by the scanning velocity (up to 5 s).

We propose that dsDNA, charged negatively in the phosphate buffer, is bound to the positively charged methylated P4VP surfaces of the nanopores. Rupture forces of similar strength have been reported before for the interaction of single dsDNA with charged surfaces.<sup>20</sup> It has also been shown that when the amphiphilic PS-*block*-P(methyl-4VP) is assembled into micelles by solvent interactions, dsDNA will be bound into the P-methyl-4VP brush by charge interactions.<sup>21</sup> Please note that our membrane is assembled in a nonsolvent-induced process, which leads to a configuration with the positively charged methylated P4VP surfaces as inner walls of the pores.

At this time, we cannot quantify the penetration of dsDNA into the pore and the length interacting with the pore wall. Suh et al. have recently investigated the role of confinement in a nanometer pore for specific binding and unbinding of a single end-functionalized polymer.<sup>22</sup> Their linker is a more flexible PEG chain, and their pore is much narrower. They show that attachment kinetics are slower, and rupture forces are lower for receptors lying deeper in the pore. The suggested effects of confinement, namely, restricted steric movement and binding orientation, will also likely limit the penetration depth and binding strength in our system. A quantification of adhesion energies at the level of single DNA molecules pulled from nanometer-scale pores in a protein crystal was reported by Wang et al.<sup>23</sup> They found an extra adhesion energy of about 30 aJ when a 30 nt DNA polymer was removed from the pore after binding to an atomic force microscope tip. Direct comparison with our force curves is difficult as the atomic force

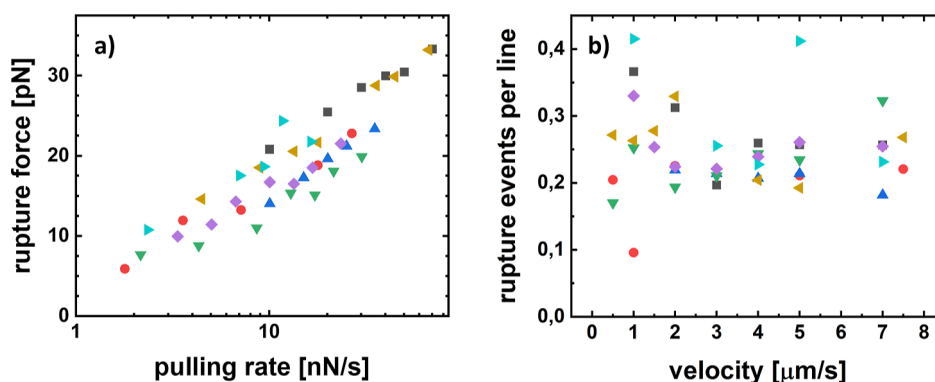


**Figure 5.** (a) Dependence of the rupture force on the pulling rate in the detachment of dsDNA from the nanoporous surface. (b) Average number of rupture events per scan line. Different colors indicate the results of seven independent implementations of the experiment.

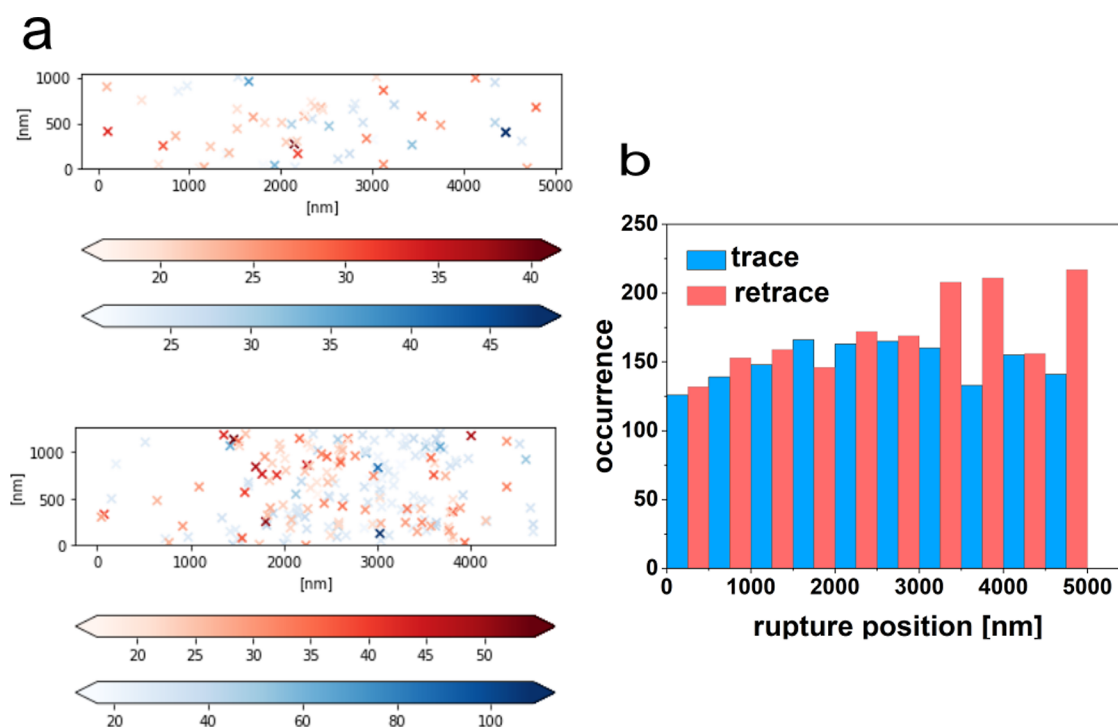


**Figure 6.** (a) Maps of the detachment events as recorded by scanning the atomic force microscope tip in two example experiments. The markers show the positions of the detachment events during trace (blue) and retrace (red). Their intensity indicates the rupture force for each detachment event (scale bars in pN). (b) Histogram of positions for all detachment events in experiments summarized in Figure 5.

microscope tip in Wang's experiment was in elastic contact with the porous crystal.

The number of detachment events per scan line is shown in Figure 5b. The number between 0.2 and 0.3 appears small when considering that the length of each scan line is 67 times the distance between pores. To further discuss the possible mechanisms of attachment, we first summarize a previous work on the role of fluctuating linker polymers in adhesion.

In their fundamental work on the role of linker length in adhesion mediated by tethered ligands, Jeppesen et al. showed that the ligand–receptor bond formation occurs in rare extensions of the linker far beyond their equilibrium conformation.<sup>24</sup> Their simulations explained the sudden formation of multiple adhesive bonds between two surfaces, where one was functionalized with tethered ligands and the other was functionalized with matching receptors. The distance at which this bond formation occurred was significantly larger than the end-to-end radius for the coiled linker but smaller than the contour length of the linker. The agreement between the experiments and results highlighted the onset of bond formation during rare excursions of the linker polymer beyond its equilibrium conformation. We assume that the observation of isolated single-molecule detachment events in our experiments can be explained similarly by a rare bond formation between the fluctuating dsDNA molecule and the porous membrane.

With its length of 7198 nts, our dsDNA can be considered a model polymer<sup>25</sup> for which the average end-to-end radius can be estimated as  $R_e = \sqrt{2P_L L_0} = 225$  nm, with a contour length of  $L_0 = 2448$  nm and a persistence length of  $P_L = 10.3$  nm for our dsDNA construct with nicks.<sup>12</sup> In the experiment, the height of the dsDNA attachment is nominally 250 nm, more than the expected end-to-end radius of dsDNA. We thus expect that conditions for the formation of a strong interaction

between dsDNA and a methylated pore are met rather infrequently.

We estimate the characteristic time for a bond formation with a formula derived by Bell and Terentjev who have calculated the time for bond formation across a gap as the mean first passage time for the tethered ligand over the gap as<sup>26</sup>

$$\tau = \frac{2R_G^2 d^2}{3\pi^2 D e^2} \frac{1}{1 + 36d^4/\pi^2 R_G^2} e^{3(d^2+a^2)/2R_G^2} \quad (1)$$

Entering a gap width of  $d = 250$  nm, a radius of gyration of  $R_G = 1/\sqrt{6}R_e = 100$  nm, and a capture radius of the pores of  $\epsilon = 40$  nm, we obtain a time scale of  $\tau = 7$  ms, assuming a lateral displacement of  $a = 0$  nm of the pore with respect to the polymer. We extrapolated a diffusion coefficient of  $D = 3 \times 10^8$  nm<sup>2</sup>/s based on ref 27 for the diffusion of a free monomer in the spirit of the Rouse model, as suggested in ref 26. The characteristic time scale for reaching the surface increases only by 25% if the polymer is displaced laterally with respect to the pore by half the distance between pores  $a = 37.5$  nm. Dividing the distance between pores of 75 nm by a sliding velocity of 1  $\mu$ m/s, we find that the tip passes one pore every 7.5 ms so that the fluctuating polymer typically reaches the membrane once per pore position. With one rupture event per 4 lines, it takes about 270 passages of the fluctuating polymer across the gap to bind to the membrane surface, presumably by interacting with the walls of a pore.

Figure 5b shows that the number of rupture events per line does not depend on the velocity, except for a slight increase below 2  $\mu$ m/s. For the higher velocities, the attachment probability is not a constant of time but is a constant of the distance covered by the scanning tip. This observation could be explained by a low density of binding sites, which need to

be approached by the scanning tip for attachment. Alternatively, the constant number of rupture events could be explained by a preferred attachment at the turning points of the scan movement. Figure 6 shows that we have neither observed accumulation of detachments, indicating preferred attachment positions nor any deviation from an equal distribution of detachment positions across the scan range indicating preferred attachment at the turning points. Apparent tendencies for preferred detachment in certain regions of maps in Figure 6a are misleading, as the average of several experiments leads to an even distribution.

We thus suggest the following picture of the attachment process. At scan velocities of 2  $\mu\text{m/s}$  and higher, we expect less than one extension of the fluctuating polymer to come into contact with the membrane surface per passing of each pore. At these higher velocities, the probability to bind the polymer into a pore is proportional to the scan distance as only the scanning movement will match the rare extensions of the polymer with the position of a pore. At scan velocities of 1  $\mu\text{m/s}$  and below, the fluctuating polymer probes each pore at least once and more often at even lower velocities. In this velocity regime, the number of attachments per scan line will increase with decreasing velocity. This tendency can be recognized in Figure 5b.

We motivated our study with our long-term goal to measure the contribution of single fluctuating polymers to the friction on hydrogels or on surface-grafted polymer brushes. The force curves we have observed resemble those reported in a pioneering study by Okijama et al., who pulled single poly(ethylene glycol) (PEG) polymers from poly(acrylamide) (PAA) gels of varying cross-linker density.<sup>28</sup> In that study, functionalized PEG polymers had been prepared with the PAA gel and then picked up by the atomic force microscope tip for single-molecule force spectroscopy. Friction force microscopy with single polymers on hydrogels will require us to transfer our results for the attachment in pores to the intermittent entanglement of fluctuating polymers with the hydrogel network.

## CONCLUSIONS

The friction contribution of a single fluctuating polymer, which is attached to a scanning tip and interacts intermittently with nanometer-scale pores of a membrane, was measured by AFM. Excursions of the polymer beyond its coiled equilibrium size lead to isolated events of binding of the polymer to the inner wall of a pore. The lifetime of the charge-based bond between dsDNA and methylated pore wall is long on the time scale of our experiment, i.e., several seconds. At higher lateral scan velocities, the number of binding events per scan distance is constant if it is the scanning motion that leads to a positional matching of polymer and binding pore. At lower lateral scan velocities, the number of binding events per distance increases with decreasing velocity as the fluctuating polymer explores each pore several times per passing. This experiment not only quantifies the interaction between dsDNA and methylated pores but also establishes a platform for the measurement of entanglement-related frictional forces of single polymers when replacing the membrane with a hydrogel surface.

## AUTHOR INFORMATION

### Corresponding Author

Roland Bennewitz – INM—Leibniz Institute for New Materials, 66123 Saarbrücken, Germany; Department of

Physics, Saarland University, 66123 Saarbrücken, Germany; [orcid.org/0000-0002-5464-8190](https://orcid.org/0000-0002-5464-8190); Phone: +49 681 9300213; Email: [roland.bennewitz@leibniz-inm.de](mailto:roland.bennewitz@leibniz-inm.de)

## Authors

Kordula Schellhuber – INM—Leibniz Institute for New Materials, 66123 Saarbrücken, Germany; Department of Physics, Saarland University, 66123 Saarbrücken, Germany

Johanna Blass – INM—Leibniz Institute for New Materials, 66123 Saarbrücken, Germany

Hanna Hübner – Polymer Chemistry, Saarland University, 66123 Saarbrücken, Germany

Markus Gallei – Polymer Chemistry, Saarland University, 66123 Saarbrücken, Germany; Saarene, Saarland Center of Energy Materials and Sustainability, 66123 Saarbrücken, Germany; [orcid.org/0000-0002-3740-5197](https://orcid.org/0000-0002-3740-5197)

Complete contact information is available at:

<https://pubs.acs.org/10.1021/acs.langmuir.3c03190>

## Notes

The authors declare no competing financial interest.

## ACKNOWLEDGMENTS

R.B. thanks Nicholas D. Spencer for many years of guidance through numerous scientific discussions and fruitful suggestions.

## REFERENCES

- (1) Klein, J. Shear, Friction, and Lubrication Forces Between Polymer-Bearing Surfaces. *Annu. Rev. Mater. Sci.* **1996**, *26*, 581–612.
- (2) Grest, G. S. Interfacial sliding of polymer brushes: A molecular dynamics simulation. *Phys. Rev. Lett.* **1996**, *76*, 4979–4982.
- (3) Lee, S.; Muller, M.; Ratoi-Salagean, M.; Voros, J.; Pasche, S.; De Paul, S. M.; Spikes, H. A.; Textor, M.; Spencer, N. D. Boundary lubrication of oxide surfaces by Poly(L-lysine)-g-poly(ethylene glycol) (PLL-g-PEG) in aqueous media. *Tribol. Lett.* **2003**, *15*, 231–239.
- (4) Müller, M.; Lee, S.; Spikes, H. A.; Spencer, N. D. The influence of molecular architecture on the macroscopic lubrication properties of the brush-like co-polyelectrolyte poly(L-lysine)-g-poly(ethylene glycol) (PLL-g-PEG) adsorbed on oxide surfaces. *Tribol. Lett.* **2003**, *15*, 395–405.
- (5) Drobek, T.; Spencer, N. D. Nanotribology of surface-grafted PEG layers in an aqueous environment. *Langmuir* **2008**, *24*, 1484–1488.
- (6) Müller, M. T.; Yan, X. P.; Lee, S. W.; Perry, S. S.; Spencer, N. D. Lubrication properties of a brushlike copolymer as a function of the amount of solvent absorbed within the brush. *Macromolecules* **2005**, *38*, 5706–5713.
- (7) Meier, Y. A.; Zhang, K. H.; Spencer, N. D.; Simic, R. Linking Friction and Surface Properties of Hydrogels Molded Against Materials of Different Surface Energies. *Langmuir* **2019**, *35*, 15805–15812.
- (8) Simić, R.; Yetkin, M.; Zhang, K. H.; Spencer, N. D. Importance of Hydration and Surface Structure for Friction of Acrylamide Hydrogels. *Tribol. Lett.* **2020**, *68*, 64.
- (9) Goren, T.; Spencer, N. D.; Crockett, R. Impact of chain morphology on the lubricity of surface-grafted polysaccharides. *RSC Adv.* **2014**, *4*, 21497–21503.
- (10) Yan, W. Q.; Ramakrishna, S. N.; Spencer, N. D.; Benetti, E. M. Brushes, Graft Copolymers, or Bottlebrushes? The Effect of Polymer Architecture on the Nanotribological Properties of Grafted-from Assemblies. *Langmuir* **2019**, *35*, 11255–11264.
- (11) Yang, D.; Ward, A.; Halvorsen, K.; Wong, W. P. Multiplexed single-molecule force spectroscopy using a centrifuge. *Nat. Commun.* **2016**, *7*, 11026.

(12) Penth, M.; Schellnhuber, K.; Bennewitz, R.; Blass, J. Nanomechanics of self-assembled DNA building blocks. *Nanoscale* **2021**, *13*, 9371–9380.

(13) Gallei, M.; Rangou, S.; Filiz, V.; Buhr, K.; Bolmer, S.; Abetz, C.; Abetz, V. The Influence of Magnesium Acetate on the Structure Formation of Polystyrene-block-poly(4-vinylpyridine)-Based Integral-Asymmetric Membranes. *Macromol. Chem. Phys.* **2013**, *214*, 1037–1046.

(14) Balzer, B. N.; Gallei, M.; Hauf, M. V.; Stallhofer, M.; Wiegler, L.; Holleitner, A.; Rehahn, M.; Hugel, T. Nanoscale Friction Mechanisms at Solid-Liquid Interfaces. *Angew. Chem., Int. Ed.* **2013**, *52*, 6541–6544.

(15) Kienle, S.; Gallei, M.; Yu, H.; Zhang, B. Z.; Krysiak, S.; Balzer, B. N.; Rehahn, M.; Schluter, A. D.; Hugel, T. Effect of Molecular Architecture on Single Polymer Adhesion. *Langmuir* **2014**, *30*, 4351–4357.

(16) Kawai, S.; Benassi, A.; Gnecco, E.; Sode, H.; Pawlak, R.; Feng, X. L.; Mullen, K.; Passerone, D.; Pignedoli, C. A.; Ruffieux, P.; Fasel, R.; Meyer, E. Superlubricity of graphene nanoribbons on gold surfaces. *Science* **2016**, *351*, 957–961.

(17) Zhang, Z.; Rahman, M. M.; Abetz, C.; Bajer, B.; Wang, J.; Abetz, V. Quaternization of a Polystyrene-block-poly(4-vinylpyridine) Isoporous Membrane: An Approach to Tune the Pore Size and the Charge Density. *Macromol. Rapid Commun.* **2019**, *40*, 1800729.

(18) Cai, W. H.; Trefs, J. L.; Hugel, T.; Balzer, B. N. Anisotropy of  $\pi$ - $\pi$  Stacking as Basis for Superlubricity. *ACS Mater. Lett.* **2023**, *5*, 172–179.

(19) Evans, E. Probing the relation between force - Lifetime - and chemistry in single molecular bonds. *Annu. Rev. Biophys. Biomol. Struct.* **2001**, *30*, 105–128.

(20) Erdmann, M.; David, R.; Fornof, A.; Gaub, H. E. Electrically controlled DNA adhesion. *Nat. Nanotechnol.* **2010**, *5*, 154–159.

(21) Yang, C.-H.; Yang, P.-W.; Lin, T.-L.; Jeng, U. S. The adsorption of DNA by cationic core-shell diblock copolymer polystyrene-block-poly(N-methyl 4-vinylpyridine iodide) micelles. *Colloids Surf., B* **2019**, *176*, 325–333.

(22) Suh, S. H.; Xing, Y.; Rottensteiner, A.; Zhu, R.; Oh, Y. J.; Howorka, S.; Hinterdorfer, P. Molecular Recognition in Confined Space Elucidated with DNA Nanopores and Single-Molecule Force Microscopy. *Nano Lett.* **2023**, *23*, 4439–4447.

(23) Wang, D. F.; Stuart, J. D.; Jones, A. A.; Snow, C. D.; Kipper, M. J. Measuring interactions of DNA with nanoporous protein crystals by atomic force microscopy. *Nanoscale* **2021**, *13*, 10871–10881.

(24) Jeppesen, C.; Wong, J. Y.; Kuhl, T. L.; Israelachvili, J. N.; Mullah, N.; Zalipsky, S.; Marques, C. M. Impact of polymer tether length on multiple ligand-receptor bond formation. *Science* **2001**, *293*, 465–468.

(25) Tree, D. R.; Muralidhar, A.; Doyle, P. S.; Dorfman, K. D. Is DNA a Good Model Polymer? *Macromolecules* **2013**, *46*, 8369–8382.

(26) Bell, S.; Terentjev, E. M. Kinetics of Tethered Ligands Binding to a Surface Receptor. *Macromolecules* **2017**, *50*, 8810–8815.

(27) Petrov, E. P.; Ohrt, T.; Winkler, R. G.; Schwille, P. Diffusion and segmental dynamics of double-stranded DNA. *Phys. Rev. Lett.* **2006**, *97*, 258101.

(28) Okajima, T.; Tao, X. M.; Azehara, H.; Tokumoto, H. Force spectroscopy on single polymer incorporated into polymer gels. *J. Nanosci. Nanotechnol.* **2007**, *7*, 790–795.

## Recommended by ACS

### Timing of Phagosome Maturation Depends on Their Transport Switching from Actin to Microtubule Tracks

Yanqi Yu, Yan Yu, *et al.*

OCTOBER 23, 2023

THE JOURNAL OF PHYSICAL CHEMISTRY B

READ 

### Metal-Induced Energy Transfer (MIET) Imaging of Cell Surface Engineering with Multivalent DNA Nanobrushes

Dong-Xia Wang, Tao Chen, *et al.*

JANUARY 17, 2024

ACS NANO

READ 

### Rapid Electrohydrodynamic-Driven Pattern Replication over a Large Area via Ultrahigh Voltage Pulses

Hyunje Park, Dae Joon Kang, *et al.*

NOVEMBER 08, 2023

ACS NANO

READ 

### Diffusion of Knotted DNA Molecules in Nanochannels in the Extended de Gennes Regime

Zixue Ma and Kevin D. Dorfman

APRIL 20, 2021

MACROMOLECULES

READ 

Get More Suggestions >